Open-loop experiments of resonator micro-optic gyro*

ZHANG Xu-lin (张旭琳) [1, 2**], **and ZHOU Ke-jiang (周柯江)** [3]

1. College of Electronic Science and Technology, Shenzhen University, Shenzhen 518060, China

2. Shenzhen Key Laboratory of Micro-Nano Photonic Information Technology, Shenzhen 518060, China

3. Department of Information Science and Electronic Engineering, Zhejiang University, Hangzhou 310027, China

(Received 15 October 2008)

An open-loop resonator micro-optic gyro (R-MOG) with a 6 cm-long waveguide-type ring resonator is set up using the phase modulation spectroscopy technique. In the experiment, according to the test parameters of the resonator, the shot-noise-limited sensitivity is estimated to be 1.07×10^{-4} rad/s. From the test demodulation signal, the gyro dynamic range of $\pm7.0\times10^{3}$ rad/s is obtained. Using different phase modulation frequencies, the open-loop gyro output signal is observed when the equivalent gyro rotation is applied to the acoustic-optical modulators (AOMs). The sensitivity of the R-MOG can be increased by some countermeasures against system noise.

Document code: A **Article ID:** 1673-1905(2009)02-0097-4

DOI 10.1007/s11801-009-8144-5

Resonator optic gyros (ROGs) based on the Sagnac effect[1] have been proposed and investigated over the past years, which is a frequency-sensitive device. ROGs have been developed as attractive devices for many navigation and guidance applications[2]. ROG with short-length ring about 5-10 m will construct the same grade as for interferometer optic gyro with 1 km length coil. Resonator micro-optic gyro (R-MOG) with an only several-cm-long ring is a promising candidate for the next generation inertial rotation[3]. Ma H et al proposed a novel silica waveguide ring resonator with single-turn[4] and the one with multi-turn structure[5]. Hsiao H et al presented another type of ring resonator on planar glass waveguide[6]. They all focused on the structure and characteristics of the ring resonator.

In this paper, an open-loop operation R-MOG system is presented in experiment. The gyro output signal with the equivalent rotation rate is achieved by the phase modulation (PM) spectroscopy technique [7] using the $LiNbO_3$ phase modulators [8]. In the PM spectroscopy technique, the $LiNbO_3$ phase modulators are used to integrate with other optical devices easily, such as the integrated micro-optic resonator. They will make the R-MOG system smaller[3].

Supposed that the R-MOG is rotating in the CW direction, the relationship between the rotation rate Ω and the Sagnac frequency difference ΔF based on the Sagnac effect[1] is reported as

$$\Delta F = f_{\text{CCW}} - f_{\text{CW}} = \frac{D}{n_0 \lambda} \Omega \quad , \qquad (1)$$

where f_{CCW} and f_{CW} refer to the resonance frequencies of the resonator in counter-clockwise (CCW) and clockwise (CW) direction, respectively. D and n_0 are the diameter and the index of ring resonator, respectively. λ is the wavelength of the laser.

Fig.1 shows the experimental schematic diagram of the R-MOG.

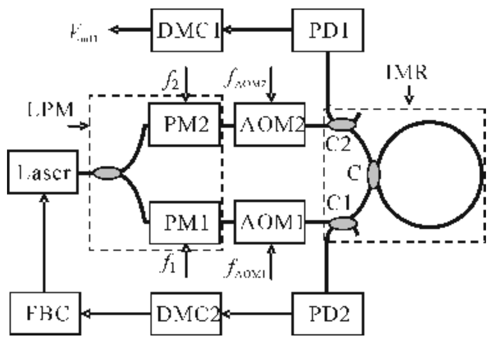

Fig.1 Structural diagram of the R-MOG

The integrated micro-optic resonator (IMR) is the key sensing part in R-MOG. In Fig.1, IMR is composed of a 6 cm-length waveguide ring, a coupler (C) with the coupling index of 5% and two couplers (C1/C2) with the coupling index of 50%. D is 2 cm, n_0 is 1.45 and λ is 1550 nm. So,

* This work has been supported by Shenzhen University Research Development Fund (No. 200867) and Shenzhen Key Laboratory of Micro-Nano Photonic Information Technology (No. 2000812).

** E-mail: zxlin@szu.edu.cn

according to Eq.(1), the scale-factor of this system is 8.9×10^3 Hz (rad/s). The output light from the laser is split into two beams with the same intensity and each beam is sine wave phase modulated by the $LiNbO_3$ phase modulators (LPM) before being injected into the resonator. The two modulation frequencies f_1 and f_2 applied to the modulators PM1 and PM2 respectively are set different to attenuate the backscattering noise[9]. The acoustic-optical modulator (AOM1) between PM1 and C1 is used to change the lightwave frequency in the CCW direction. And AOM2 between PM2 and C2 is used to change the lightwave frequency in the CW direction. The working frequencies in the CW and CCW directions, f_0^{CW} and f_0^{CCW}, are written as

$$f_0^{\mathrm{CW}} = f_0 + f_{\mathrm{AOM1}} \ , \tag{2}$$

$$f_0^{\mathrm{CCW}} = f_0 + f_{\mathrm{AOM2}} \ , \tag{3}$$

where f_0 is the frequency of the laser. f_{AOM1} and f_{AOM2} are the frequency shifts induced by AOM1 and AOM2, respectively.

The CW and CCW lightwaves in the resonator are sensed in reflection mode by photodiodes PD1 and PD2 respectively. The signals from PD1 and PD2 are demodulated by the demodulation circuits DMC1 and DMC2. The output signal from DMC1 and DMC2 can be expressed as[7]:

$$V_{out} = P\sum_n J_n(M) J_{n+1}(M) \times \\ \left[h_n h_{n+1}\sin(\phi_{n+1}-\phi_n) - h_{-n}h_{-(n+1)}\sin\left(\phi_{-n}-\phi_{-(n-1)}\right)\right] , \tag{4}$$

where h_n is the amplitude of resonator transmission function, ϕ_n is the phase of resonator transmission function, M is the modulation index, and P is a constant related to the system parameters. Eq.(4) shows the relationship between the demodulation signal V_{out} and the resonance frequency deviation Δf[7]. For the CW lightwaves,

$$\Delta f = f_0^{\mathrm{CW}} - f_{\mathrm{CW}} \ , \tag{5}$$

where f_0^{CW} is the working frequency in CW direction.

For the CCW lightwaves,

$$\Delta f = f_0^{\mathrm{CCW}} - f_{\mathrm{CCW}} \ , \tag{6}$$

where f_0^{CCW} is the working frequency in CCW direction.

In the CCW direction, the demodulation curve from DMC2 is fed back to the laser by the feedback circuit (FBC), as shown in Fig.1. f_0^{CCW} is locked to f_{CCW} by the demodulation curve from DMC2[7]. The open-loop gyro signal is observed from DMC1, V_{out1}. When the R-MOG is at rest, $f_{\mathrm{CW}}=f_{\mathrm{CCW}}$. While the R-MOG is rotating, there is a Sagnac frequency difference ΔF between f_{CW} and f_{CCW} [1].

According to Eq.(2) and Eq.(3), Eq.(6) is rewritten as

$$\Delta f = f_{\mathrm{CCW}} - f_{\mathrm{AOM2}} + f_{\mathrm{AOM1}} - f_{\mathrm{CW}} = \\ (f_{\mathrm{AOM1}} - f_{\mathrm{AOM2}}) + (f_{\mathrm{CCW}} - f_{\mathrm{CW}}) \ . \tag{7}$$

Compared Eq.(1) and Eq.(7), Eq.(7) is rewritten as

$$\Delta f = (f_{\mathrm{AOM1}} - f_{\mathrm{AOM2}}) + \Delta F \ . \tag{8}$$

From Eq.(8), it's known that the difference between f_{AOM1} and f_{AOM2} induced by AOM1 and AOM2 is equivalent to the Sagnac frequency difference ΔF caused by the gyro rotation.

According to the theoretical analysis above, an experimental system of R-MOG is set up to measure the equivalent gyro output caused by the difference between f_{AOM1} and f_{AOM2} induced by AOM1 and AOM2. The structural diagram of the experimental system is similar to Fig.1, and the parameters of the integrated micro-optic resonator are the same with those theoretical values in Fig.1. The modulation frequencies f_1 and f_2 are 17 MHz and 30 MHz, respectively, and the modulation index is about 2.405[7].

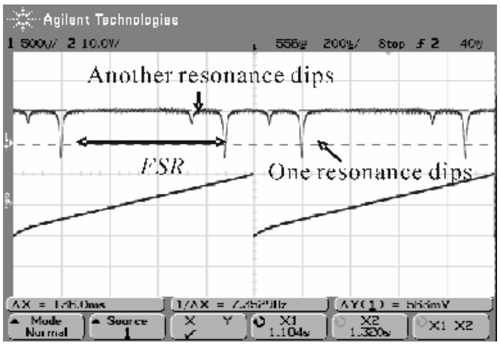

Fig.2 Upper curve is the resonance curve of the resonator and the lower curve is the low frequency sawtooth-wave voltage applied to the laser.

Firstly, the resonance curve of the resonator is tested. A low frequency sawtooth-wave voltage is applied to the laser. The lasing frequency f_0 will change linearly with time. The applied voltage is a sawtooth-wave with amplitude of 20 V and period of 1 s, as shown in the lower curve of Fig.2. Since f_0 changes linearly with the input voltage at 0.25 GHz/V, f_0 changes linearly with time at 5.0 G/s by this sawtooth wave. The oscilloscope trace of the upper curve in Fig.2 shows the resonance curve in the CW direction. According to the time spaces in the upper curve of Fig.2, the free spectral range of the resonator (FSR), the full width at half maximum of the resonance curve (FWHM) and the fineness (F) of the resonator are measured as 3.1 GHz, 52 MHz and 60 MHz. According to these test values, it can be estimated that the shot-noise-limited sensitivity of this system is 1.07×10^{-4} rad/s [9]. There are two resonance dips with different depths in the upper curve of Fig.2, because two eigenstates of polarization (ESOPs) exist in the resonator[10]. The resonance dip with smaller depth is the noise to the one with larger depth.

Fig.3 shows the demodulation signals from DMC1 and DMC2, respectively. The lower curve of Fig.3 is used to make the CCW loop lock-in, while the upper one is the open-loop output signal. According to the upper curve of Fig.3, the amplitude and the time space corresponding to the linear part of the demodulation curve are 22.5 V and 25 ms, respectively. Since f_0 changes linearly with time at 5.0 G/s by the sawtooth wave in Fig.2, the linear part of the demodulation curve in the lower curve of Fig.2 is ±62.5 MHz. The dynamic range of this R-MOG is $\pm7.0\times10^3$ rad/s because of the scale-factor about 8.9×10^3 Hz (rad/s). The slope of the linear part in the demodulation signal from DMC1 is estimated to be 1.6 mV (rad/s) from Fig.3.

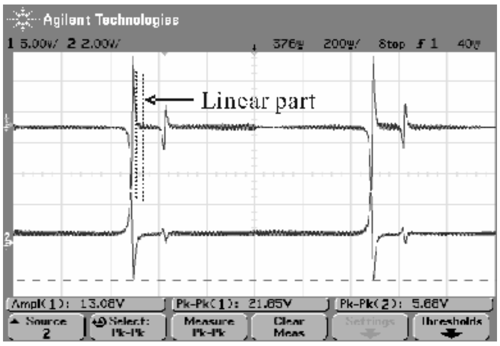

Fig.3 Upper curve is the demodulation signal from DMC1, while the lower curve is that from DMC2.

After obtaining the demodulation signal of the R-MOG, the open-loop system is set up. Two frequency shifts f_{AOM1} and f_{AOM2} are applied to AOM1 and AOM2, respectively. When f_{AOM1}-f_{AOM2} is ±0.5 MHz, the equivalent rotation rate is ±112.4 rad/s theoretically, because of the scale-factor about 8.9×10^3 Hz (rad/s). Since the slope of the linear part in the upper curve of Fig.3 is 1.6 mV(rad/s), the gyro output signal corresponding to the equivalent rotation rate with ±112.4 rad/s is estimated to be 179.8 mV. In the experiment, when f_0^{CCW} is locked to f_{CCW}, the open-loop gyro output with equivalent rotation rate is observed from DMC1, as shown in Fig.4. f_{AOM2} is 40 MHz. f_{AOM1} increases from 40 MHz to 40.5 MHz directly, and then reduces to 40 MHz. It means that f_{AOM1}-f_{AOM2} is 0.5 MHz, which corresponds to equivalent rotation rate at 112.4 rad/s in the CW direction. The open-loop signal with equivalent rotation rate is 131.3 mV, as shown in the first half part of Fig.4. In the other half part of Fig.4, it shows the open-loop signal when f_{AOM1} reduces from 40 MHz to 40. 5 MHz directly, then increases to 40 MHz. And f_{AOM1}-f_{AOM2} = -0.5 MHz, which is equivalent to rotation rate at 112.4 rad/s in the CCW direction. From the other half part of Fig.4, it's known that the equivalent gyro signal is 96.6 mV. The difference between the test and estimation is because that when the frequency shift by the AOM is larger or smaller than 40 MHz, the excess insertion loss of the AOM will increase. Especially, 3 dB excess insertion loss occurs at approximately 40 MHz ±3 MHz.

The middle part of the curve in Fig.4 corresponding to f_{AOM1} = 40 MHz shows the drift characteristics of the R-MOG in 3.6 s. The bias drift is approximately 60 mV. It refers to the rotation rate of 37.5 rad/s, which is larger than the shot-noise-limited sensitivity of 1.07×10^{-4} rad/s. As a preliminary experiment, only two different modulation frequencies are taken to attenuate the backscatter errors[9]. Other noise sources in the system, such as polarization and Kerr effect[10] have not made countermeasures to overcome.

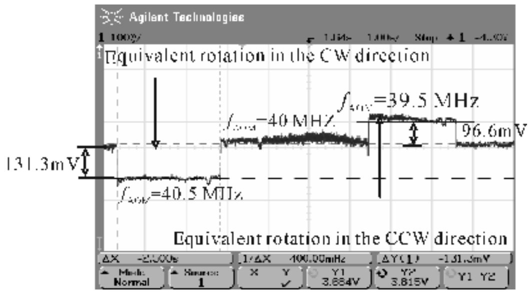

Fig.4 Open-loop gyro signal with equivalent rotation rate from DMC1.

In conclusion, an open-loop operation R-MOG system is set up by the phase modulation spectroscopy scheme using the $LiNbO_3$ phase modulators. When f_0^{CCW} is locked, the driving frequency difference of the two AOMs is equivalent to the Sagnac frequency deviation proportional to the rotation rate of the R-MOG. The equivalent gyro output signal is gotten in the open-loop experiment. Calculated from the demodulation signal, the dynamic range of the gyro is from $+7.0\times10^3$ rad/s to -7.0×10^3 rad/s. And from the test parameters of the resonator, the shot-noise-limited sensitivity of the R-MOG system is estimated to 1.07×10^{-4} rad/s. In the future, the gyro sensitivity could be increased by taking some action to overcome the error sources.

References

[1] Post E J, Review of Modern Physics, 39 (1967), 475.

[2] Barbour N and Schmidt G, IEEE Sensors Journal, **1** (2001), 332.

[3] Suzuki K, Takiguchi K and Hotate K, Journal of Lightwave Technology, **18** (2000), 66.

[4] Ma Huilian, Jin Zhonghe, Ding Chun and Wang Yuelin, Chinese Journal of Lasers, **32** (2005), 1330 (in Chinese)

[5] Ma Huilian, Wang Shijun and Jin Zhonghe, Optics Communications, **281** (2008), 2509.

[6] Hsiao H and Winick K A, Optics Express, **15** (2007), 17783.

[7] Zhang Xulin, Ma Hulian, Ding Chun, Chinese Journal of Lasers, **32** (2005), 85(in Chinese)

[8] Hotate K and Harumoto M, Journal of Lightwave Technology, **15** (1997), 466

[9] Iwatsuki K, Hotate K and Higashiguchi M, Applied Optics, 23 (1984), 3916.

[10] Hotate K and Takiguchi K, SPIE, **1585** (1991), 116.